Theory and applications of hyperbolic invariant manifolds in astrodynamics

Christos Efthymiopoulos

RCAAM, Academy of Athens

Spiral arms or rings composed by chaotic orbits

Voglis, C.E. and Tsoutsis, 2006, Patsis 2006, Romero-Gomez et al. 2006, 2007,

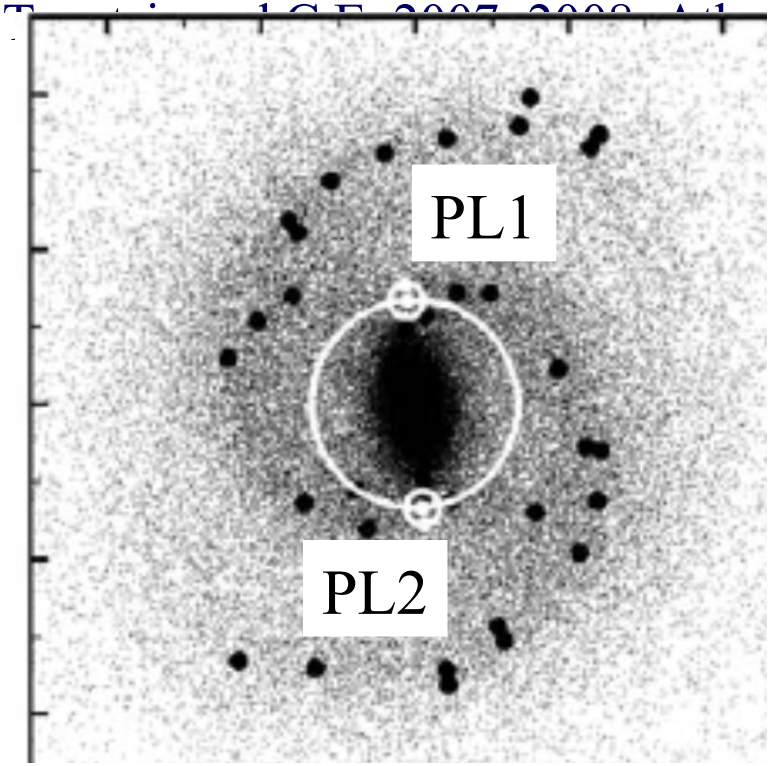

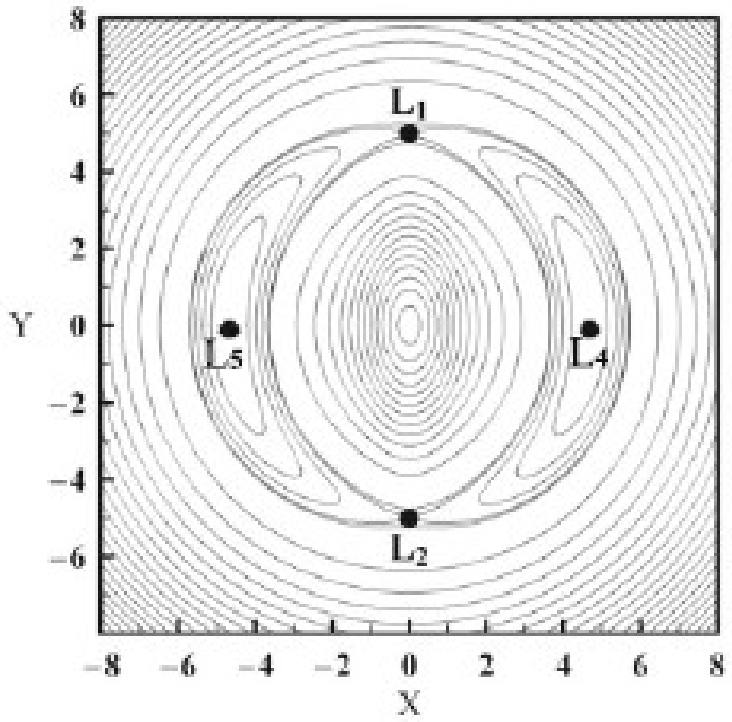

Definition of the unstable invariant manifold of PL1

$$\mathcal{W}^{U}_{PL_1} = \left[\bigcup (r_0, \theta_0, p_{r0}, p_{\theta 0}) : \lim_{t \to -\infty} ||Q(t; r_0, \theta_0, p_{r0}, p_{\theta 0}) - PL_1|| = 0 \right]$$

Invariant manifolds of the unstable short period orbits

$$H = \kappa_* I_1 + \alpha_* I_1^2 + 2b_* I_1 I_2 + c_* I_2^2 + A_* \cos 2\theta_2$$
$$- \epsilon \left[\frac{2(I_1 + I_{10})}{\kappa_*} \right]^{1/2} I_2[\cos(\theta_1 + 2\theta_2) - \cos(\theta_1 - 2\theta_2)]$$

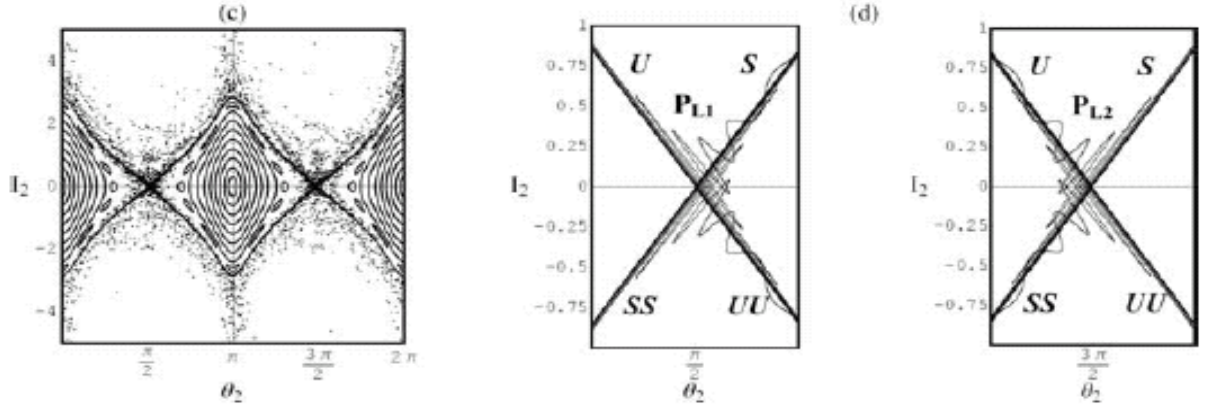

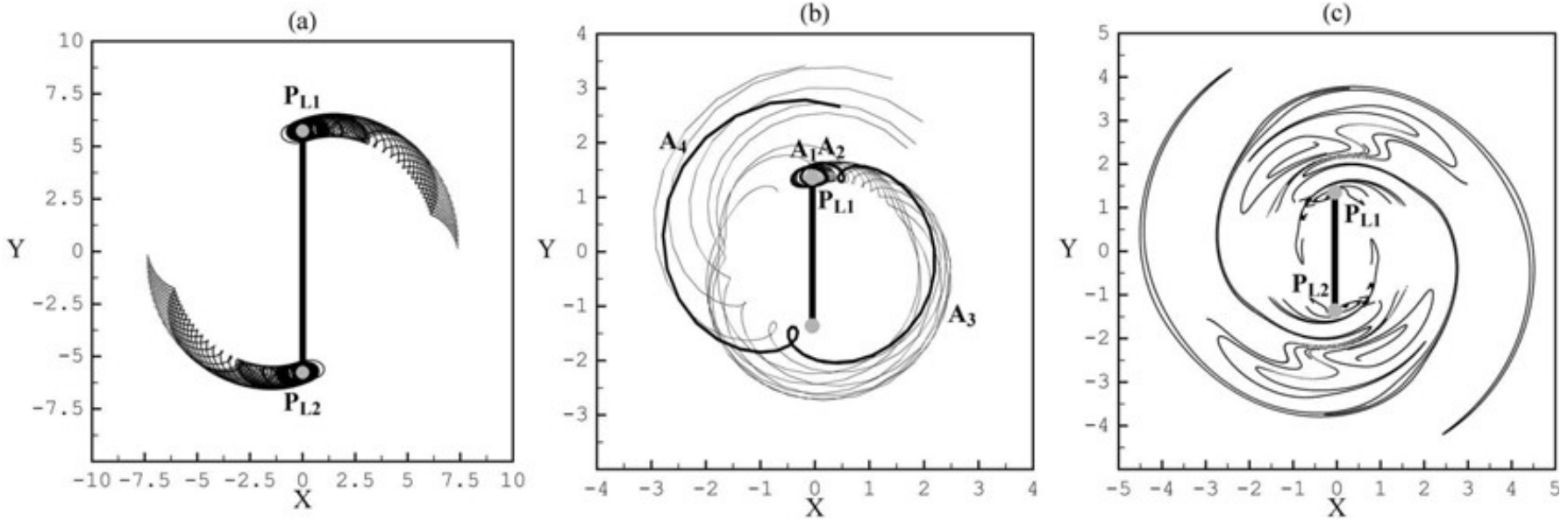

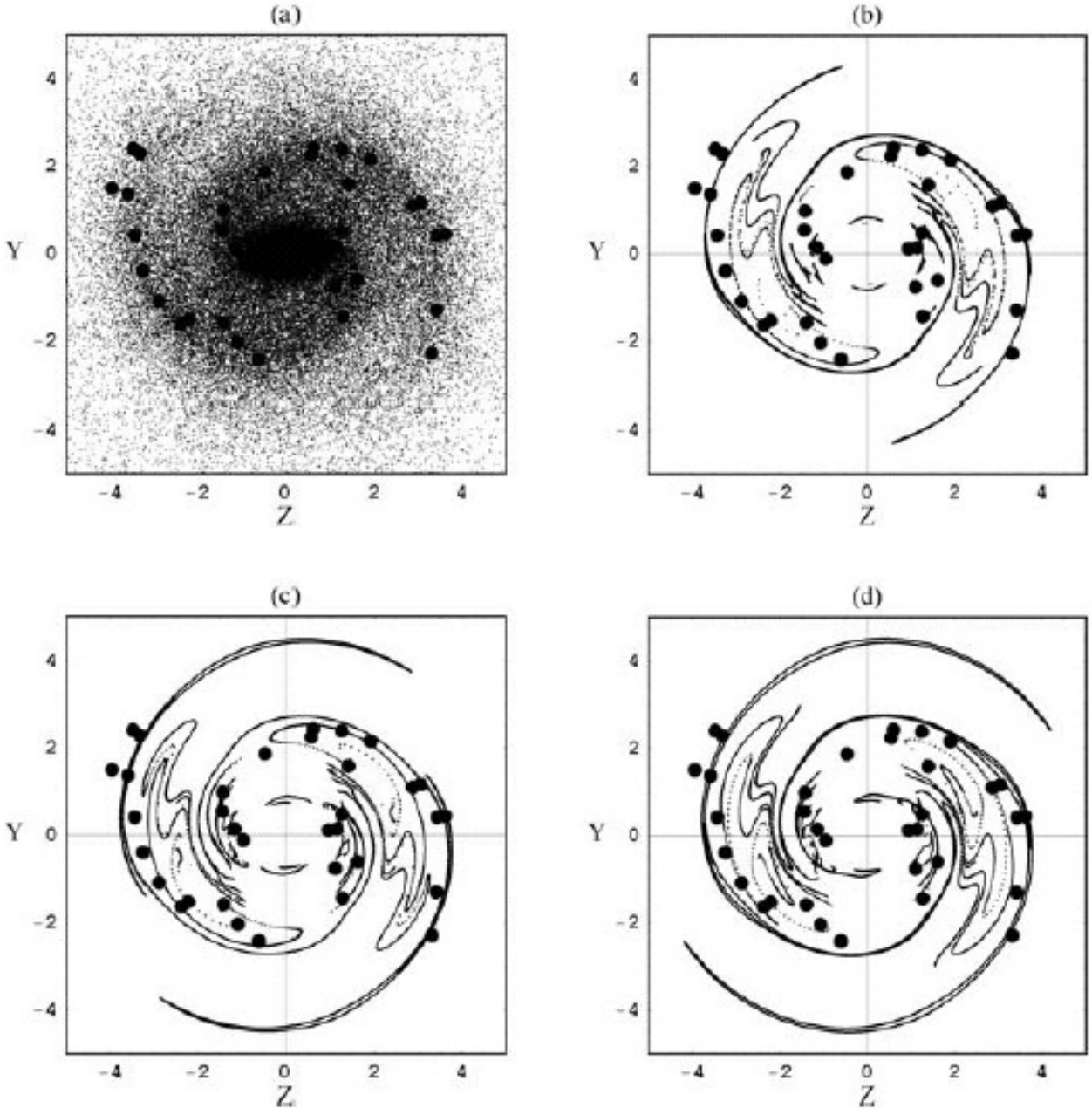
(a)
(b)
(c)
(d)
Y
Z
4
2
0
-2
-4

Coalescence of the invariant manifolds of all periodic orbits in a connected chaotic domain

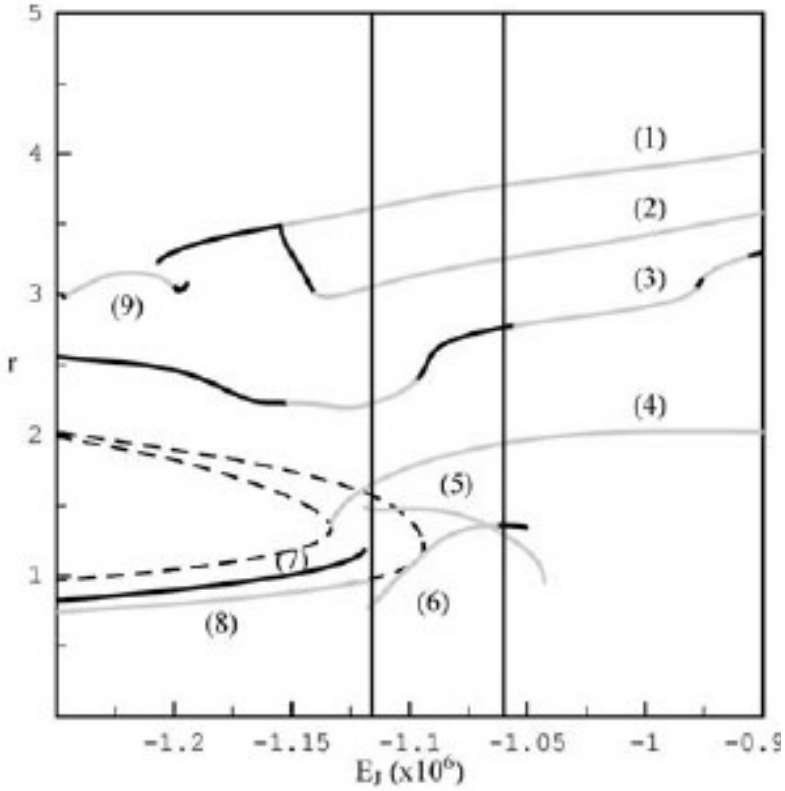

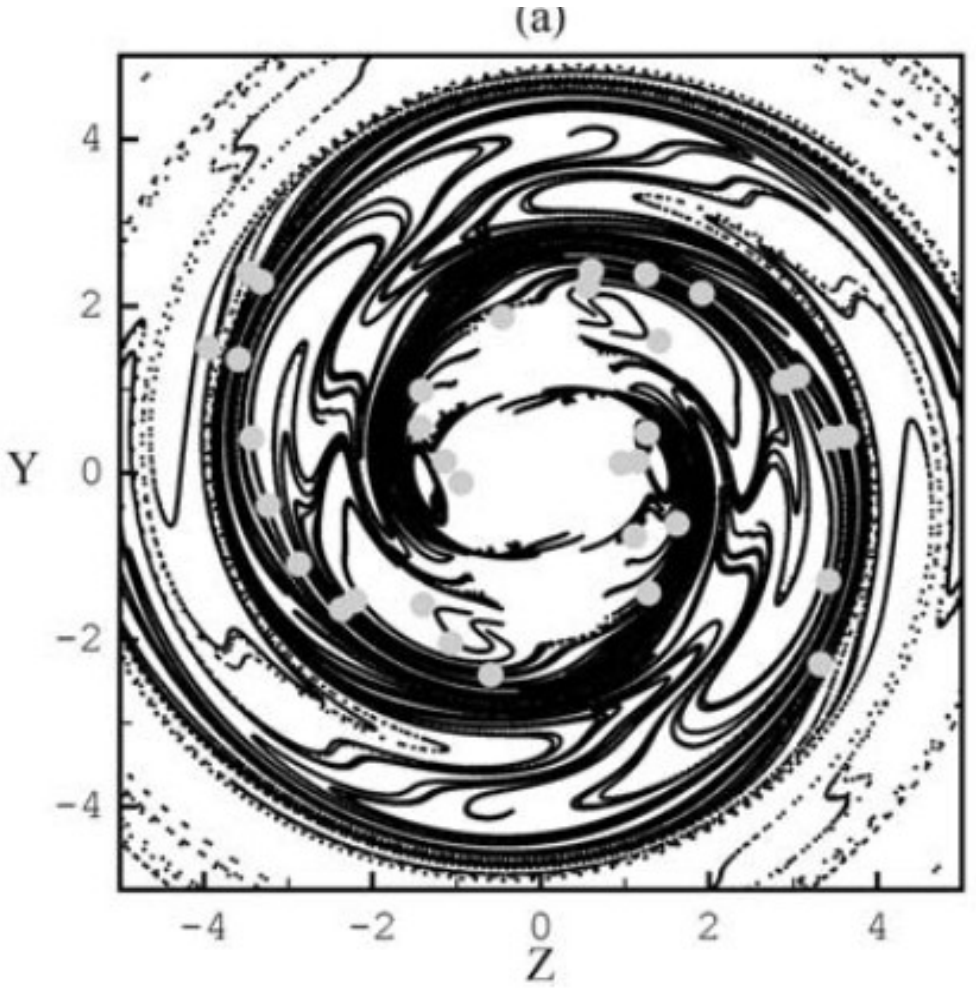

Limits of motion in the CRTBP

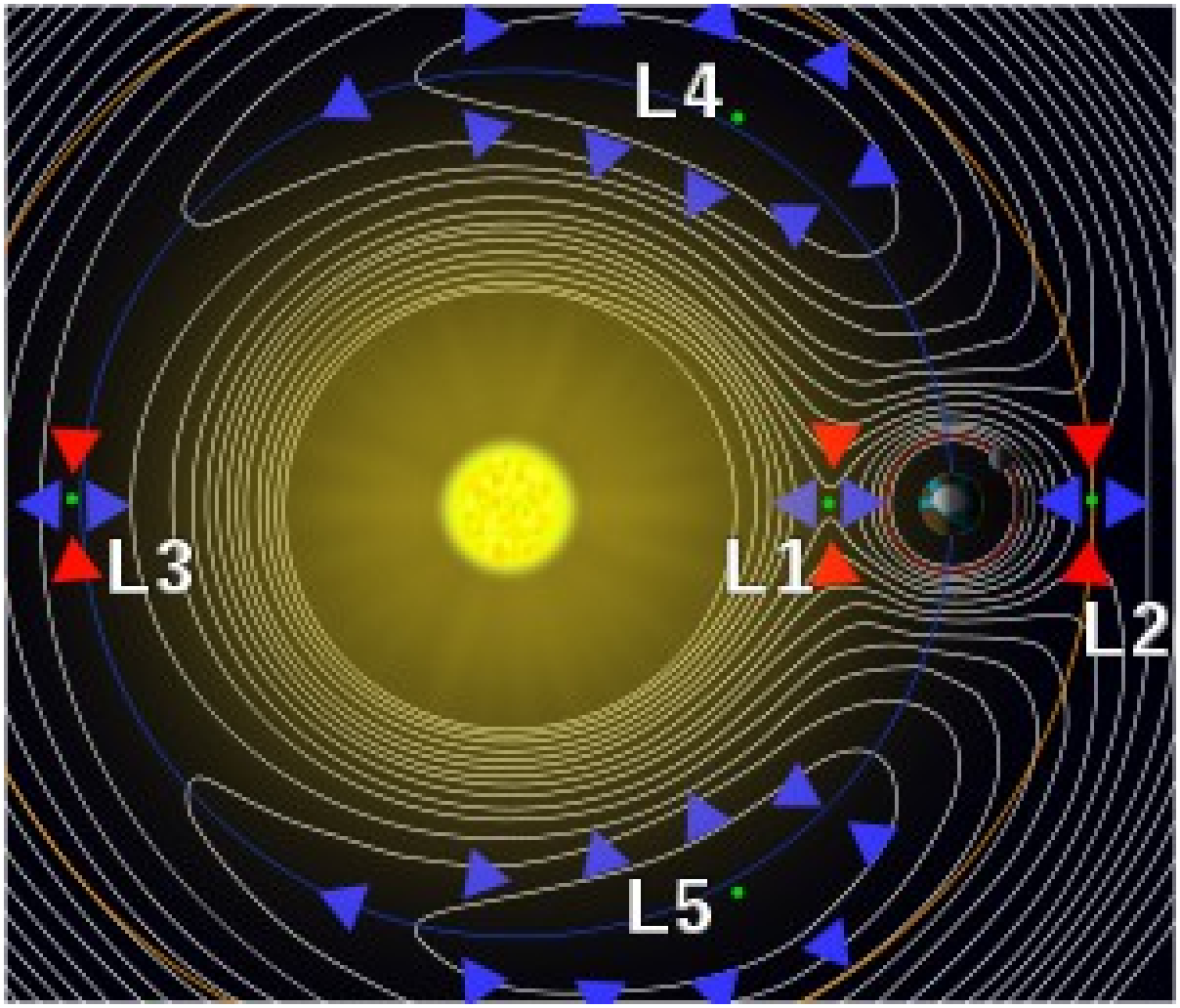

Limits of motion in the CRTBP

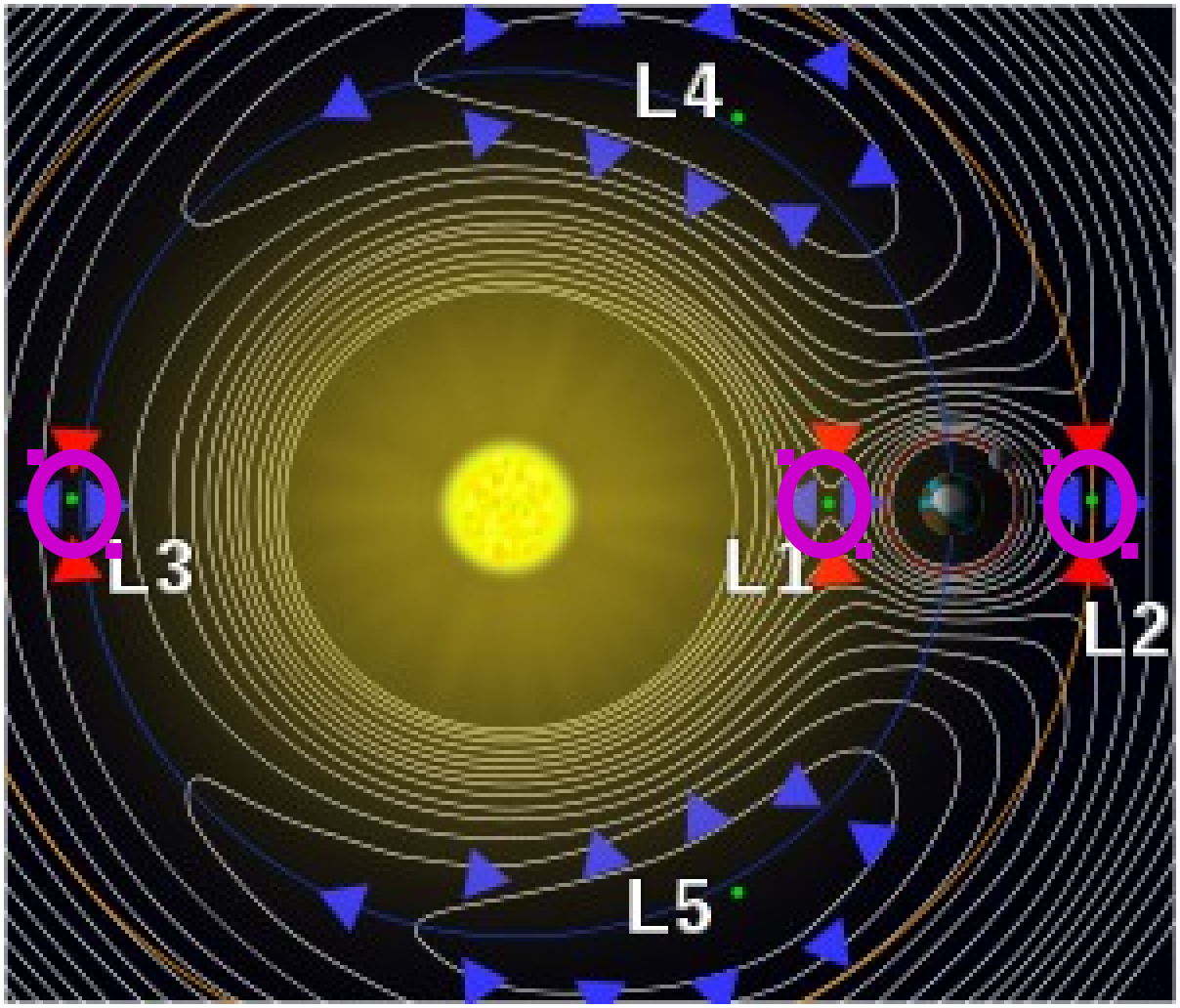

Invariant manifold tubes
(Conley 1968, Gomez et al. 1991, Koon et al. 2000)

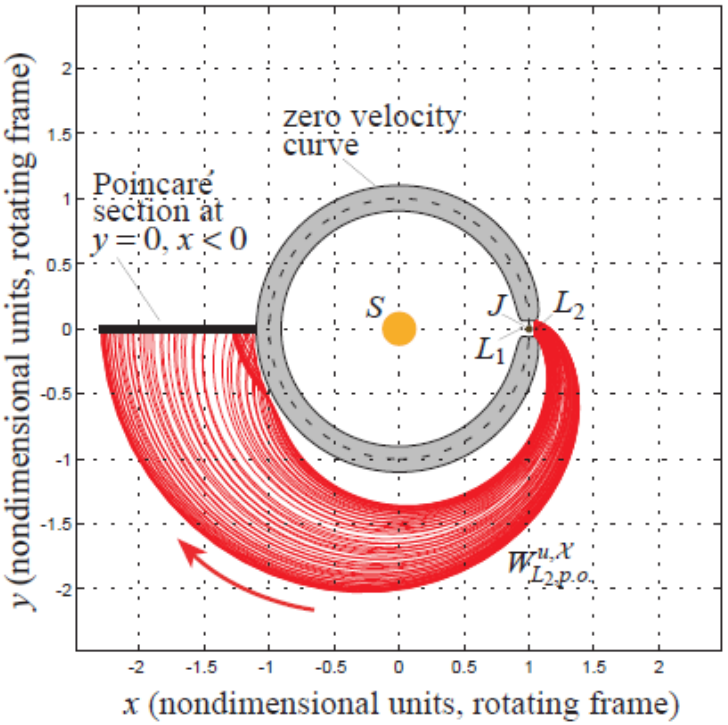

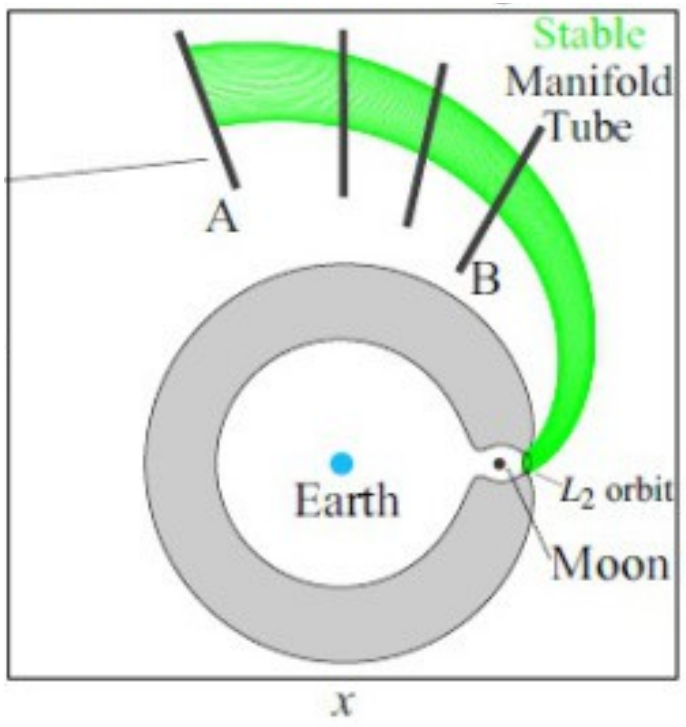

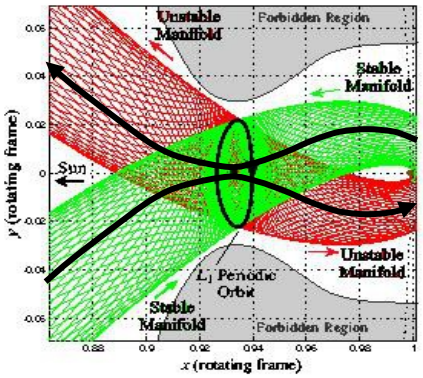

Koon et al. 2000

The successful story of "Hiten" (MUSES-B, Belbruno and Miller 1993)

low cost "fly to the moon" **through the Weak Stability Boundary**

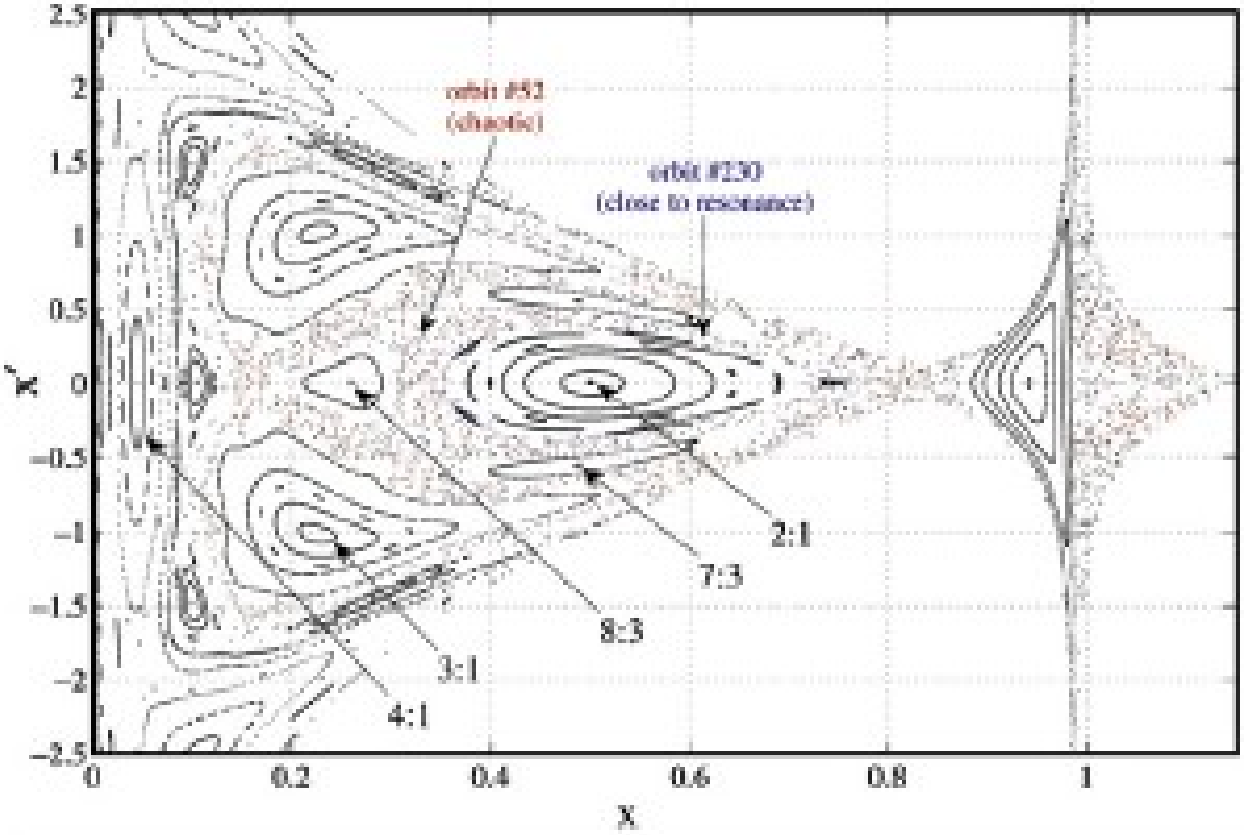

Topputo et al. 2008

Koon et al 2001: exploiting heteroclinic intersections between various "Lyapunov" orbits

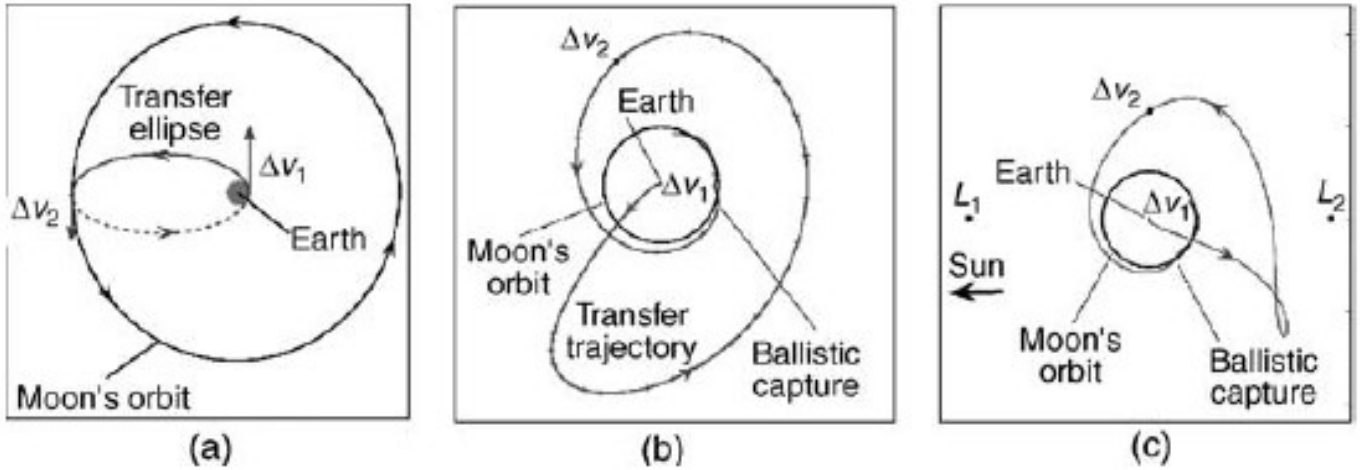

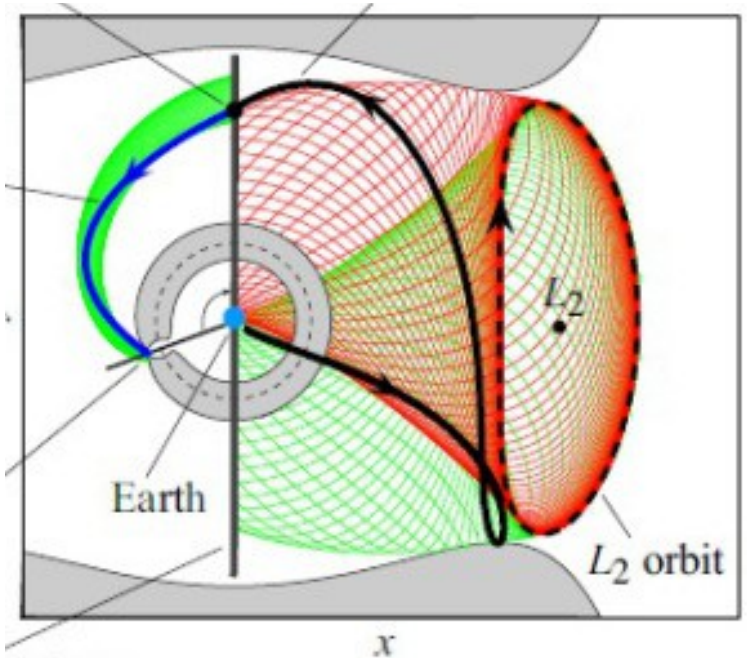

ARTEMIS low cost orbit design (2011)

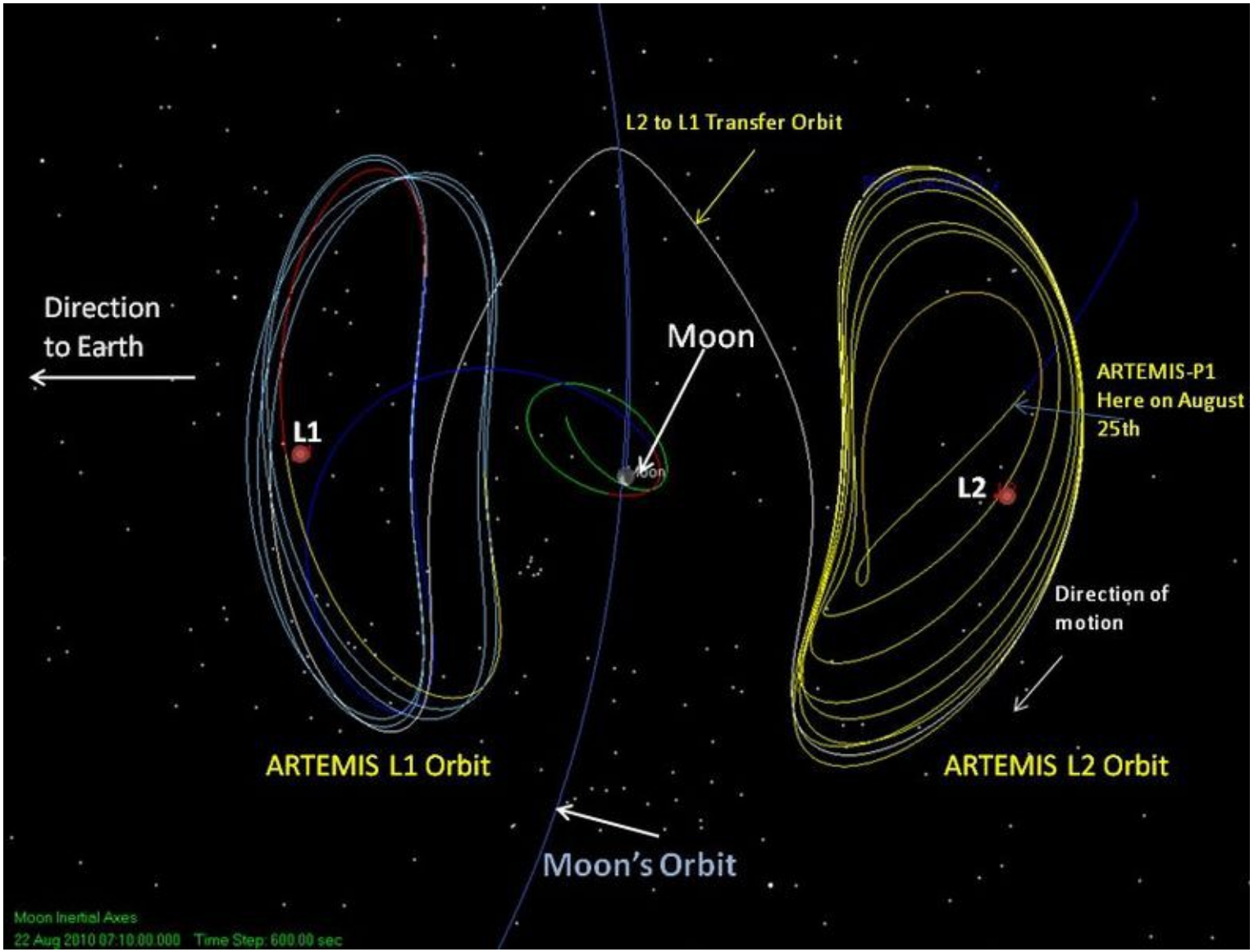

Genesis versus SOHO

SOHO (1995)

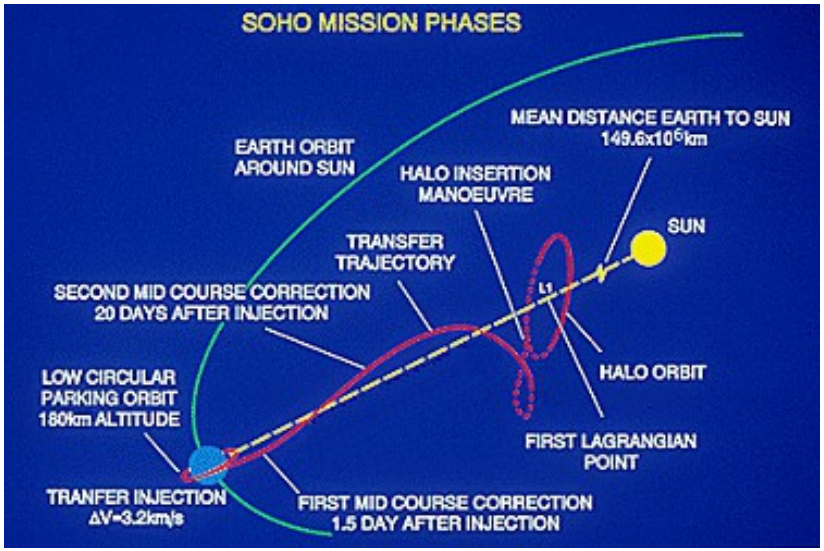

Genesis (2001)

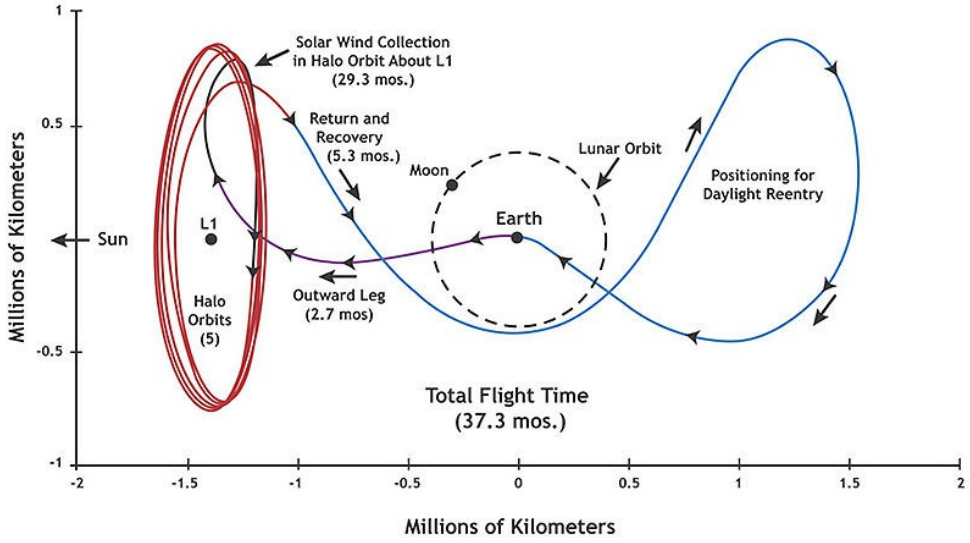

Petit Grand Tour

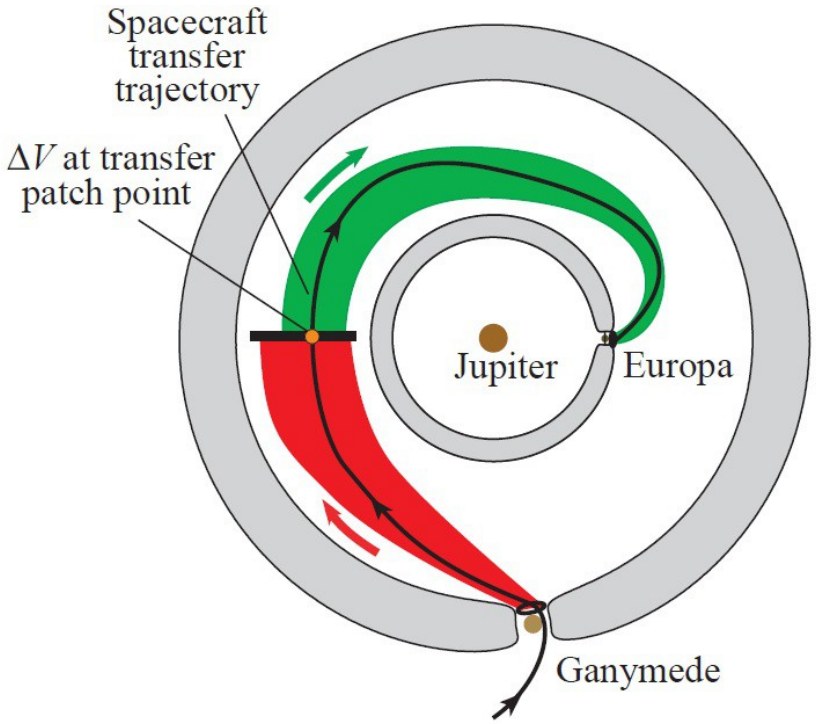

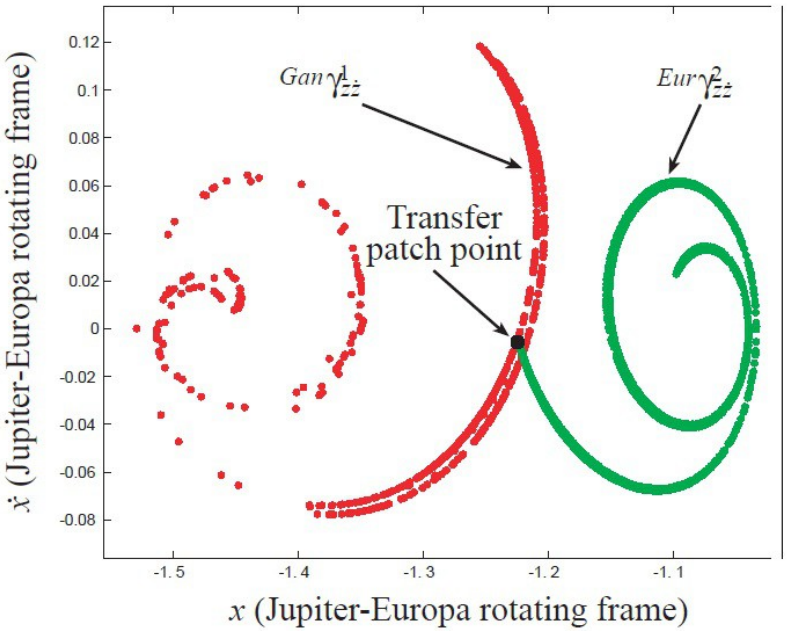

Captures, escapes, transitions and jumps of trojan asteroids (or planets in extrasolar planetary systems; Astrodynamics group Vienna + C.E., see also Koon et al. 2001b)

$\sqrt{a}-1$

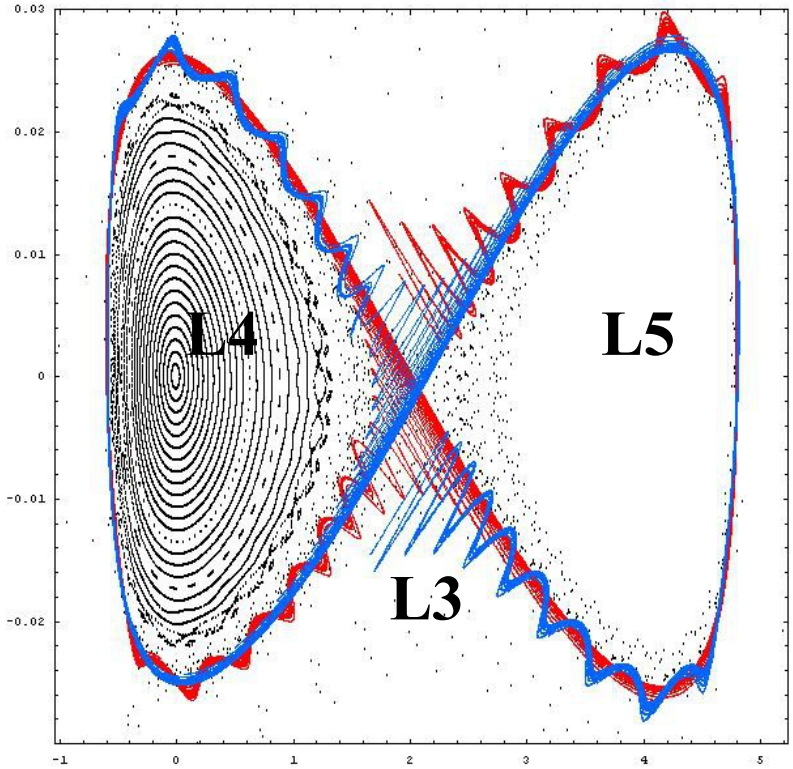

e=0.3

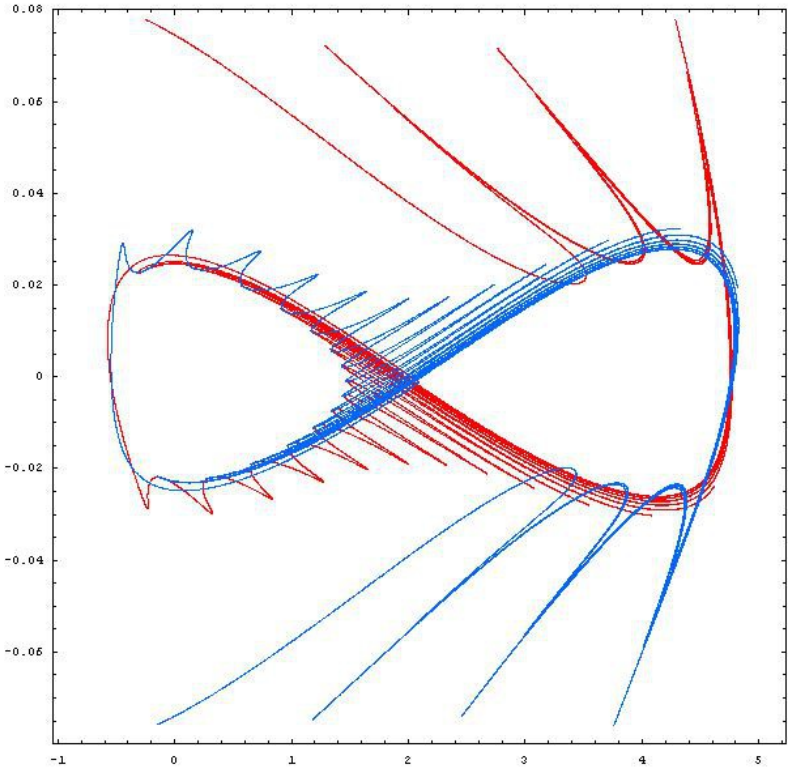

Analytical computations of invariant manifolds

$$H = \frac{p^2}{2} - \omega_0^2(1 + \epsilon(1+p)\cos\omega t)\cos\psi$$

$$H(\psi, \phi, p, I) = \frac{p^2}{2} + \omega I - \omega_0^2(1 + \epsilon(1+p)\cos\phi)\cos\psi$$

$$H = \frac{p^2}{2} + I - 0.08\left(1 + 0.5\epsilon(1+p)(e^{i\phi} + e^{-i\phi})\right)\left(-1 + \frac{u^2}{2} - \frac{u^4}{24} - \ldots\right)$$

Birkhoff - Moser variables

$$p = \frac{\sqrt{\nu}(\xi + \eta)}{\sqrt{2}}, \quad u = \frac{(\xi - \eta)}{\sqrt{2\nu}}$$

$$H(\phi, I, \xi, \eta) = \omega I + \nu\xi\eta + H_1(\phi, I, \xi, \eta)$$

Near identity canonical transformation

$$\begin{aligned}
\xi &= \Phi_\xi(\xi', \phi', \eta', I') \\
\phi &= \Phi_\phi(\xi', \phi', \eta', I') \\
\eta &= \Phi_\eta(\xi', \phi', \eta', I') \\
I &= \Phi_I(\xi', \phi', \eta', I')
\end{aligned}$$

Moser normal form (see also Giorgilli 2001, Gabré et l. 2006)

$$Z_h = \omega I' + \nu \xi' \eta' + Z(I', \xi' \eta')$$

$$\dot{\delta\xi'} = (\nu + \nu_1(I'))\delta\xi', \qquad \dot{\delta\eta'} = -(\nu + \nu_1(I'))\delta\eta'$$

Hamiltonian normalization via Lie series

$$H^{(r)} = Z_0 + \lambda Z_1 + ... + \lambda^r Z_r + \lambda^{r+1} H^{(r)}_{r+1} + \lambda^{r+2} H^{(r)}_{r+2} + \dots$$

Lie canonical transformation

$$H^{(r+1)} = \exp(L_{\chi_{r+1}}) H^{(r)}$$

New form of the Hamiltonian

$$H^{(r+1)} = Z_0 + \lambda Z_1 + ... + \lambda^r Z_r + \lambda^{r+1} Z_{r+1} + \lambda^{r+2} H^{(r+1)}_{r+2} + \dots$$

Choose terms to be normalized

$$h_{r+1}^{(r)} = \sum_{(s_1,s_2,k_2)\notin\mathcal{M}} b_{s_1,s_2,k_2}(I)\xi^{s_1}\eta^{s_2}e^{ik_2\phi}$$

Homological equation

$$\{Z_0, \chi_{r+1}\} + \lambda^{r+1}h_{r+1}^{(r)} = 0$$

$$\left\{\omega I + \nu\xi\eta, \xi^{s_1}\eta^{s_2}a(I)e^{ik_2\phi}\right\} = -[(s_1-s_2)\nu + i\omega k_2]\xi^{s_1}\eta^{s_2}a(I)e^{ik_2\phi}$$

$$\mathcal{M} = \{(s_1, s_2, k_2) : s_1 = s_2 \text{ and } k_2 = 0\} \quad .$$

$$\chi_{r+1} = \sum_{(s_1,s_2,k_2)\notin\mathcal{M}} \frac{b_{s_1,s_2,k_2}(I)}{(s_1-s_2)\nu + i\omega k_2}\xi^{s_1}\eta^{s_2}e^{ik_2\phi}$$

No small divisors!

Hamiltonian model

$$H = \frac{p^2}{2} - \omega_0^2(1 + \epsilon(1+p)\cos\omega t)\cos\psi$$

$$H(\psi, \phi, p, I) = \frac{p^2}{2} + \omega I - \omega_0^2(1 + \epsilon(1+p)\cos\phi)\cos\psi$$

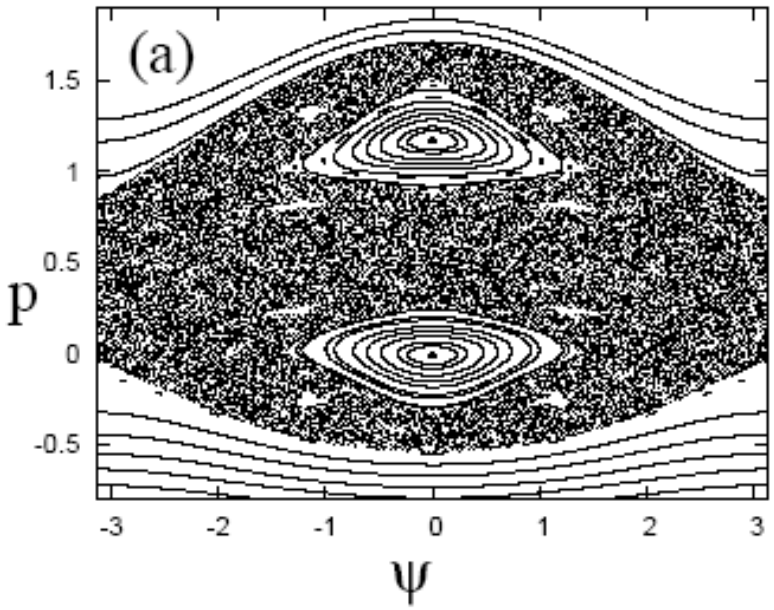

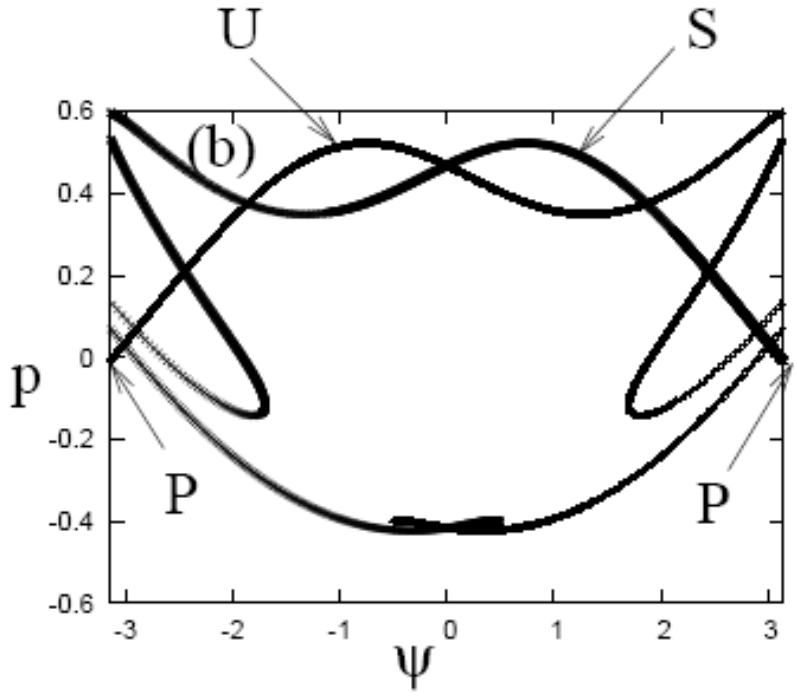

Domain of convergence

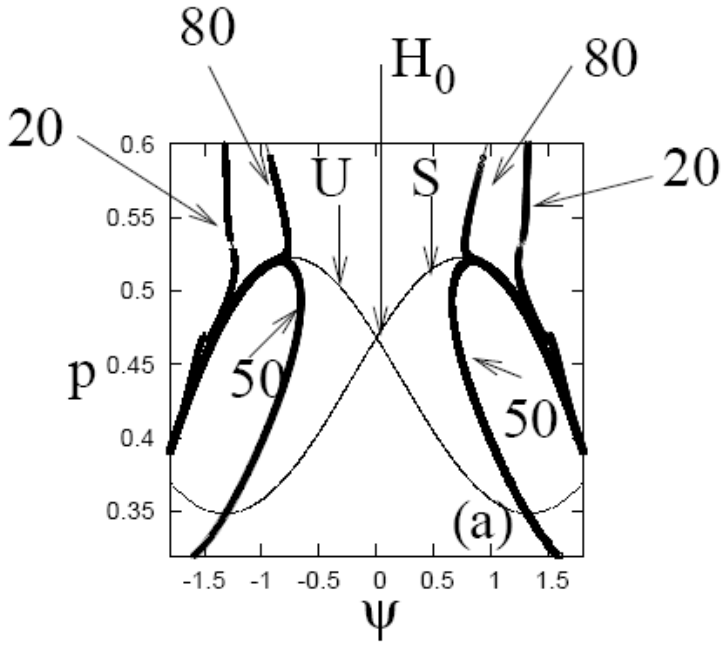

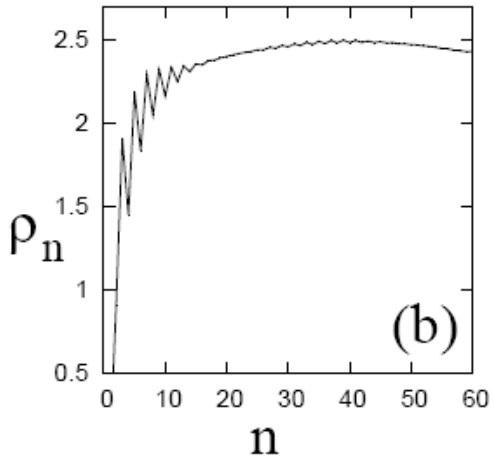

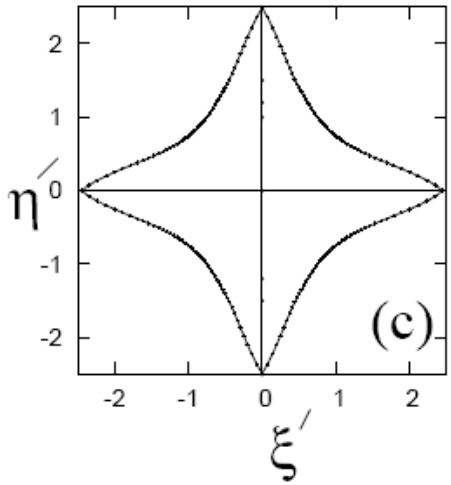

Extended Method (Efthymiopoulos et al. 2013)

$$q_t = \exp(L_{tH})q$$

$$p_t = \exp(L_{tH})p = \sum_{k_1,k_2} \tilde{f}_{p,(k_1,k_2)}(p,I,t)e^{i(k_1\psi+k_2\phi)}$$

$$\tilde{f}_{p,(k_1,k_2)}(p,I,t) = \tilde{f}^{(0)}_{p,(k_1,k_2)}(p,I) + t\tilde{f}^{(1)}_{p,(k_1,k_2)}(p,I) + t^2\tilde{f}^{(2)}_{p,(k_1,k_2)}(p,I) + ...$$

$$|\tilde{f}_{p,(k_1,k_2)}(p,I,t)| < Ae^{-(|k_1|+|k_2|)\sigma}$$

$$F_{T,S_T} = F_{t_n} \circ F_{t_{n-1}} \circ \ldots \circ F_{t_1}, \qquad S_T = \left\{ t_1, t_2, \ldots, t_n : \sum_{i=1}^{n} t_i = T \right\}$$

Extended Moser transformation

$$\Phi_m = F_T^m \circ \Phi \circ N_T^{-m}, \quad m = 0, \pm 1, \pm 2, \ldots$$

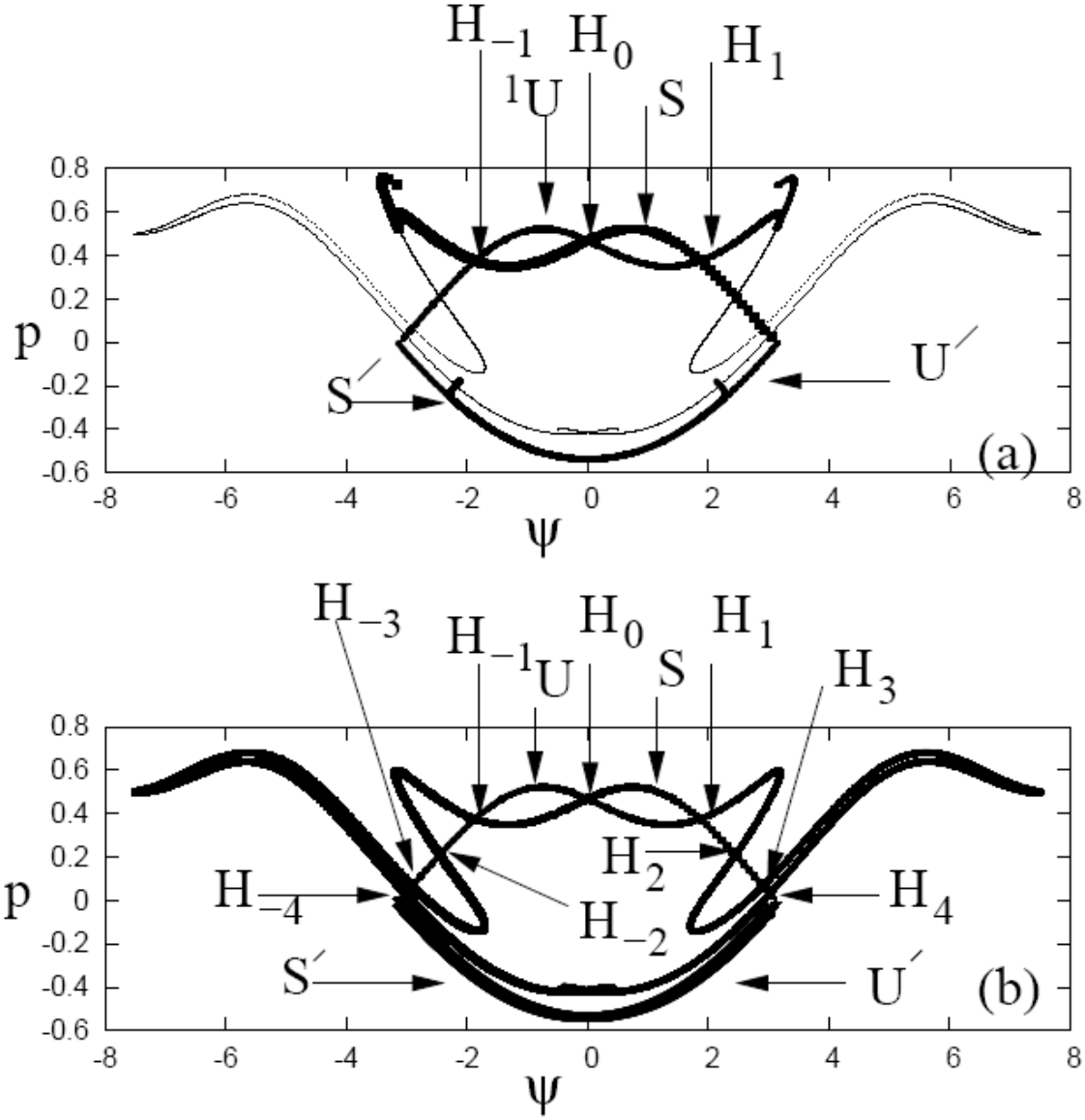
H−1
H0
H1
1U
S
S´
U´
(a)
p
ψ
H−3
H3
H2
H−4
H4
H−2
(b)

Hamiltonian polynomial model

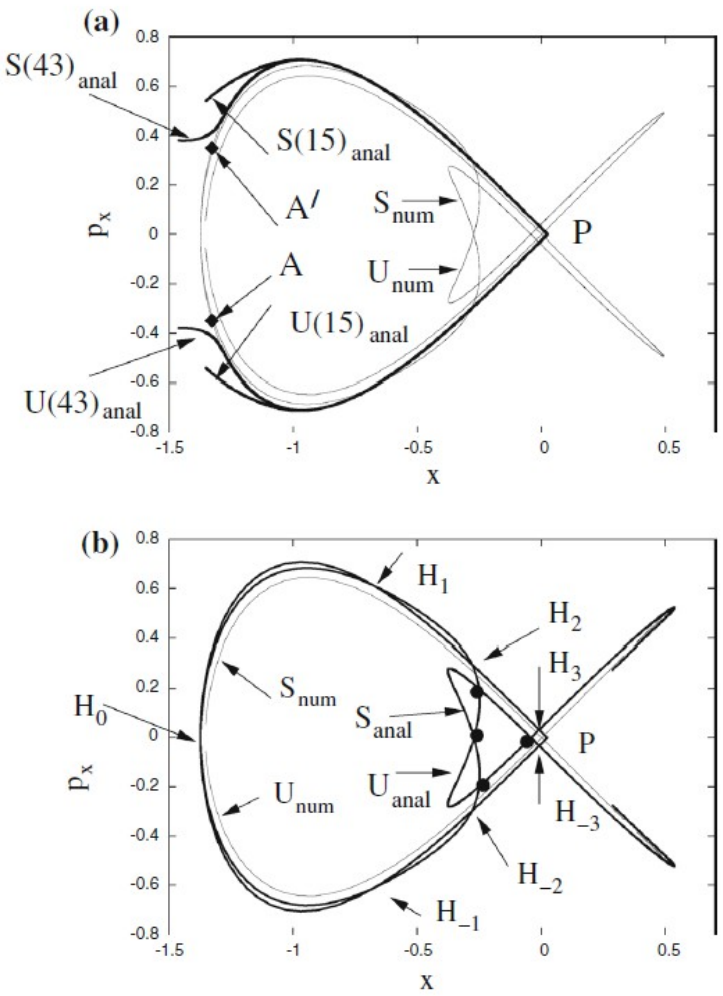

Fig. 10 **a** Analytical (*thick lines*) versus numerical (*thin lines*) invariant manifolds in the model (34), at the energy $E = 0.03$, in the surface of section given by $\phi' = 0$, for the unstable manifold, or $\phi' = \pi$ for the stable manifold, where ϕ' is the angle in the new variables in the elliptic degree of freedom after implementing the normal form transformations (see text). The analytical manifolds are computed at the truncation orders $r = 15$ and $r = 43$. The points A and A' represent the limit of convergence of the series along the unstable and stable manifolds respectively. **b** Same as in (**a**), but now with for the analytical manifolds computed by the extended method of Sect. 4. The analytical manifolds now reproduce well several lobes of the numerical ones, and they can be used to locate the position of the homoclinic points H_0 and $H_{\pm j}$, $j = 1, 2, 3$. The *thick dots* represent higher order homoclinic points reproduced by the same computation

Computation of Homoclinic points by root-finding

$$K(\xi,\eta) = p(\xi,0) - p(0,\eta) = 0, \quad L(\xi,\eta) = \psi(\xi,0) - \psi(0,\eta) = 0$$

Invariant Moser curves

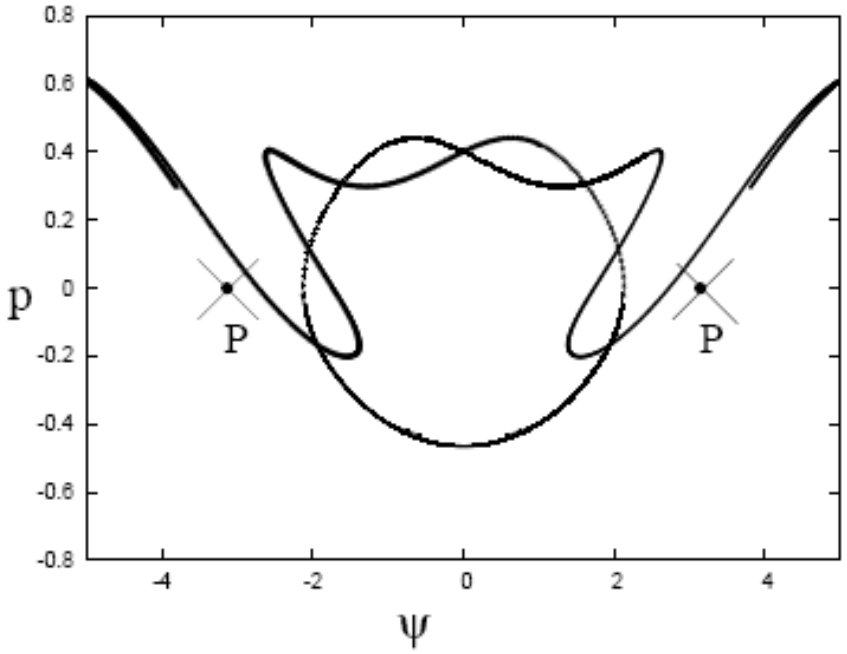

Analytic structure of chaos

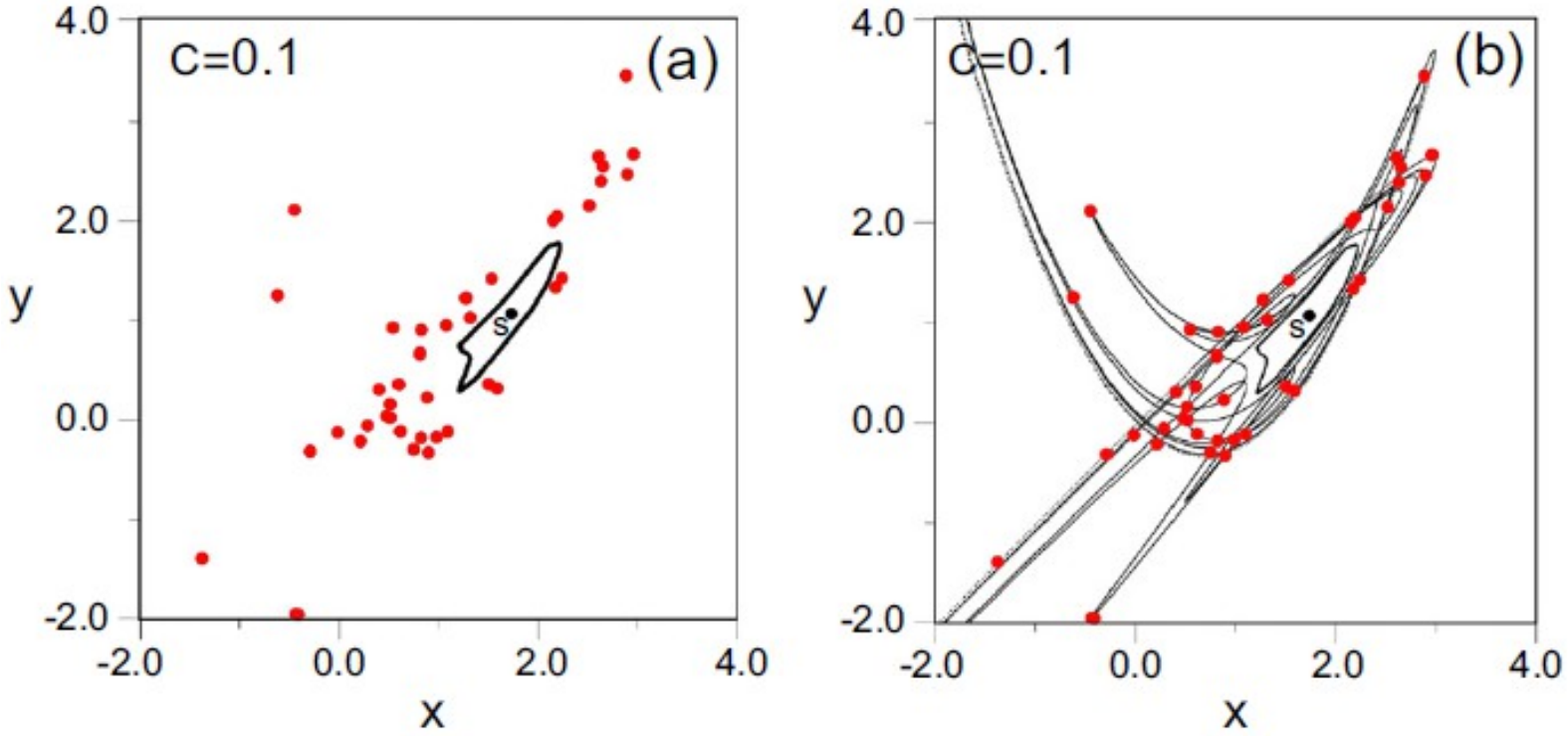

Figure 3. (a) The successive iterations of two orbits having initial points on the invariant curve $c = 0.1$ seem to be distributed randomly around the last KAM curve of a central island of stability (b) the scattered points of figure 3(a) belong in fact to the invariant curve $c = 0.1$.

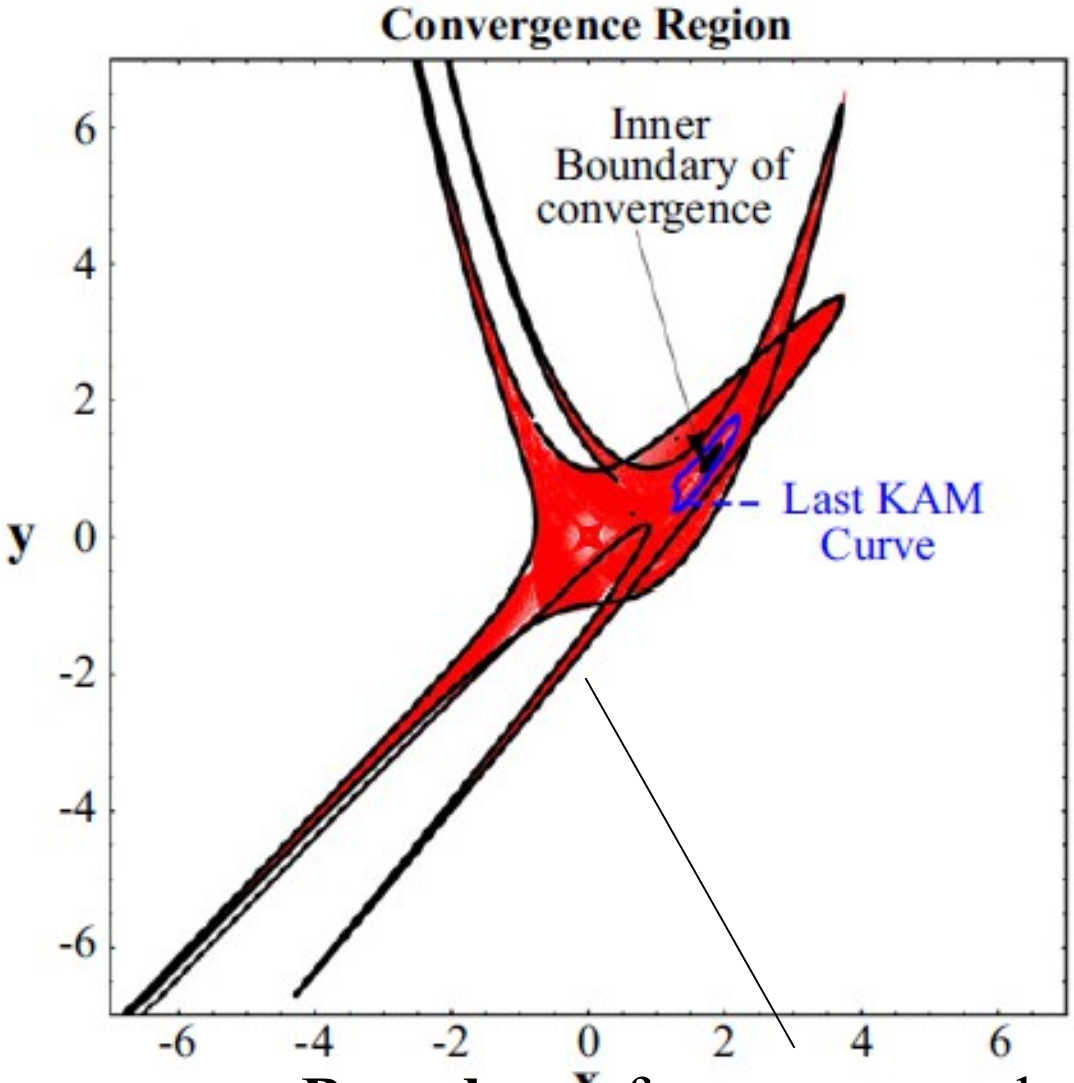

Boundary of convergence domain:
Acts as **attractor of** chaotically escaping orbits (Harsoula et al. 2015)

Conclusions

Hyperbolic invariant manifolds → orbit design via chaotic dynamics

Real missions

Analytical computation of homoclinic and heteroclinic dynamics, helpful in optimization algorithms of orbit design

Convergence issues – extended method

Other astrophysical applications (asteroid and comet dynamics, spiral structure etc.)